

Experimental Study on Spectral Reflective Properties of a Painted Layer

Hamdy M. Shafey,* Y. Tsuboi,† M. Fujita,† T. Makino,‡ and T. Kunitomo§
Kyoto University, Kyoto, Japan

A new diffuse reflectometer using a paraboloidal mirror has been developed and employed to measure various reflective properties of painted layers for the case of normal incidence. The effects of the pigment volume concentration, the scattering properties of the pigment (TiO_2 , Fe_2O_3 , carbon, and ZnO), the thickness of the painted layer, the reflection characteristics of the substrate (specular or diffuse) on the spectral normal-hemispherical reflectance, and the angular distribution of the diffuse reflection are studied. The wavelength dependence of the results is examined over the range of $0.45 \sim 10 \mu\text{m}$. The comparison with the analysis indicates that the experimental results, with the exception of the interference effect at large pigment volume concentrations, are in reasonable agreement with the analytical results.

Nomenclature

C	= correction factor
d	= pigment diameter
L	= layer thickness
M	= detector output for specular reflection measurement
n_p	= refractive index of pigment
R	= reflectivity
V	= detector output for diffuse reflection measurement
v	= volume concentration of pigment
W	= weight
x	= correction factor
γ	= specific gravity
λ	= wavelength
θ	= polar angle
θ_0	= semiapex angle of incident hole
τ_l	= optical thickness of painted layer
$\bar{\omega}$	= scattering albedo

Superscript

()^{*} = reference mirror

Subscripts

c	= dense state
D	= diffuse component
h	= hemispherical
pig	= pigment
S	= specular component
veh	= vehicle
w	= wet state

Introduction

REFLECTIVE properties of paint coatings are of particular importance for the design of various types of thermal equipment and the development of new coatings with spectrally selective radiative properties, e.g., coated surfaces for solar energy collectors and thermal control coatings for spacecraft.

Theoretical studies¹⁻⁵ have been carried out by the present authors on the radiative transfer in the general and practical

application of a painted layer to investigate the effects of various factors on its reflective properties. In these studies, the intensity of the diffuse radiation field and the intensity of the attenuated incident beam were obtained as the complementary solution and as the particular solution, respectively, of the general transfer equation. The factors considered were the shape, size, optical properties, and volume concentration of pigment, the optical properties of vehicle and substrate, and the thickness of painted layer.

Previous experimental studies⁶⁻¹² have been limited generally to the short wavelength range, simple systems of paints, and approximate measuring techniques. Usually reflectance techniques are used to measure the radiative properties of painted samples at room temperature employing a suitable diffuse reflectometer. Directional-diffuse reflectometers, operated in the direct or reciprocal mode, have been discussed widely in the literature.^{13,14} They include integrating sphere reflectometers,¹⁵ heated cavity reflectometers,¹⁶ and integrating mirror reflectometers. Integrating mirrors are used to collect diffusely reflected light in the hemisphere of reflection ($2\pi\text{-sr}$). Three types of integrating mirrors have been used: Coblenz or hemispherical mirror,^{6,17} ellipsoidal (spheroidal) mirror,¹⁸ and paraboloidal mirror.¹⁹

The primary aim of this paper is to describe a revised experimental technique to investigate various diffuse reflective properties of a painted layer using a new diffuse reflectometer. This reflectometer employs a paraboloidal mirror, and it has many advantages compared with those developed by other investigators,^{15,18,19} such as measuring in a wide range of the wavelength ($0.45 \sim 10 \mu\text{m}$) and having the facility of measuring the angular distribution of diffuse reflection. The measurements of the spectral hemispherical reflectance and the angular distribution of the diffuse reflection are carried out for the normal incidence. The effects of shape, size, optical properties, and volume concentration of the pigment, the thickness of the painted layer, and the reflection characteristics of the substrate are studied. The experimental results are compared with the calculated results based on the analyses described in Refs. 1-5, using available data regarding shape, size, and optical properties of the pigments. The purpose of the comparison is to examine if one can obtain the reflective properties with the analytical techniques for engineering predictions, and to check the various assumptions which have been considered in modeling the painted layer.

Selection and Preparation of Samples

The selection of the samples was guided by a survey of the available pigment materials that are manufactured for

Received Sept. 2, 1981; revision received Jan. 26, 1982. Copyright © American Institute of Aeronautics and Astronautics, Inc., 1982. All rights reserved.

*Graduate Student, Dept. of Engineering Science; also Assistant Lecturer, Assiut University, Assiut, Egypt. Member AIAA.

†Graduate Student, Dept. of Engineering Science.

‡Instructor, Dept. of Engineering Science.

§Professor, Dept. of Engineering Science.

engineering applications. Representative pigments were selected on the basis that they include a variety in color (absorption properties in the visible region of the spectrum) and in the shape of the pigment particle, and where optical constants are known. The selected pigments for the present study are rutile titanium dioxide (TiO_2), zinc oxide (ZnO), red iron oxide (Fe_2O_3), and carbon black. Available data for the average shape and size of these pigments were obtained from Refs. 21 and 22.

Paints of each pigment with dense concentrations were prepared by dispersing the pigment powder in the wet vehicle (alkyd resin + dryer + mineral spirit). Preliminary experiments were carried out to determine the appropriate values of the pigment volume concentration for each paint, which have a distinct effect on the measured reflectances. The required pigment volume concentration in the wet state v_w is obtained by mixing uniformly the paint of dense concentration v_c with pure vehicle of the same kind according to the weight ratio

$$\frac{W_c}{W_{veh}} = [1 + v_c (\gamma_{pig}/\gamma_{veh} - 1)] \frac{v_w}{v_c - v_w} \quad (1)$$

where γ_{pig} and γ_{veh} are the specific gravities of the pigment and the vehicle, respectively.

A specular Al substrate for each sample could be obtained by evaporating a thin opaque film of high purity Al on clean glass plates. Optically thick layers of white (TiO_2) or black (carbon) paints were used as diffuse substrates. Then painted layers of specified pigment volume concentration were adjusted to have the required thickness on the prepared substrates. This was accomplished by the use of thin film applicators having nominal sizes ranging from 50 to 500 μm . The applied painted layers were allowed to dry for three days under nearly dust free conditions. Dry painted samples were prepared in square areas 9 mm \times 9 mm for diffuse reflection measurements.

Description of the Diffuse Reflectometer

Figure 1 shows schematic plan view of the diffuse reflectometer developed in the present study. A 50-W halogen (tungsten-iodine) lamp S_1 with a filament size of 3 mm \times 2 mm is used as a light source in the visible (VIS) and near infrared (NIR) regions of the wavelength spectrum ($\lambda = 0.43 \sim 2.4 \mu\text{m}$). An infrared (IR) radiator S_2 is used with a plane mirror as a light source in the infrared region ($\lambda = 2.4 \sim 10 \mu\text{m}$). It consists of a mullite ($3\text{Al}_2\text{O}_3 \cdot 2\text{SiO}_2$) blackbody cavity with a target size of 9-mm diameter, which is heated by a 300-W silicon carbide heater. For requirement of steady conditions a dc voltage stabilizer is used in the input power circuit of the halogen lamp, while a temperature controlling silicon-controlled rectifier (SCR) unit is used in the input power circuit of the silicon carbide heater.

The light beam emitted from the light source is chopped with a 8-Hz frequency by the chopper blade C, and focused by the lens R_1 at the entrance slit of a grating-type monochromator. The entrance and exit slitwidths were set at a maximum of 3 mm. This value corresponds to a resolution of the wavelength $\Delta\lambda = 0.021 \mu\text{m}$ for $\lambda = 0.43 \sim 0.7 \mu\text{m}$, $0.084 \mu\text{m}$ for $\lambda = 0.75 \sim 4.0 \mu\text{m}$, and $0.34 \mu\text{m}$ for $\lambda = 4.2 \sim 10.0 \mu\text{m}$. The lens R_2 focuses monochromatic light in the normal direction at the sample surface within a cone whose semiapex angle is 7 deg. The sample surface is located in the focal plane of the paraboloidal mirror M_p by mounting the sample on a suitable holder which can be positioned precisely by a micrometer-operated mechanism. The mirror M_p has a 30-mm focal distance and a 120-mm i.d. at the focal plane. The hemispherically reflected light at the sample surface is incident on the paraboloidal mirror and then reflected in a wide collimated beam. This beam is reflected on the spherical mirror M_s and then focused by lens R_3 at the surface of a

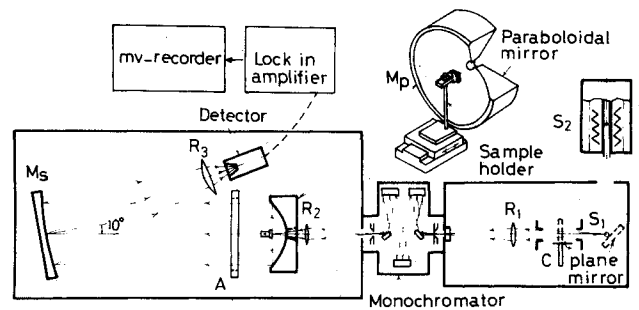


Fig. 1 Plan view of the diffuse reflectometer.

pyroelectric IR detector. Lenses of BK7 glass are used in the VIS and NIR regions, while they are replaced by lenses of KRS-5 material in the IR region. The use of lenses for focusing instead of mirrors decreases the aberration errors.

It must be noted that the specular component and a small portion of the diffuse component of the reflected light escape through the hole of incidence (in mirror M_p), and return back to the light source. This returning light is attenuated greatly due to the absorption by the light source and other optics. To avoid the multiple reflection of the stray light on the walls and the covers of the reflectometer, they are painted with anti-reflection black paint.

For measuring the polar angular distribution of the diffuse reflection a circular aperture A with varying size is located between mirrors M_p and M_s .

Measuring Procedure

For the measurement of absolute reflectance a reference quantity must be measured, which is proportional to the incident radiation energy at the sample surface. To fulfill this a reference mirror of known absolute reflectance and having the same size of the sample is used. Specular surface of evaporated Al is used as a reference mirror for measurements in the VIS region, while that of evaporated gold is used as a reference mirror in NIR and IR regions. The reflectivities of these reference mirrors are determined directly by Strong's method.²⁰ The reference mirror is mounted on a similar holder as for the sample except that its surface is inclined 20 deg to the focal plane of the paraboloidal mirror. This is done to avoid the escaping of the specularly reflected energy which is to be detected as the reference quantity. Furthermore it was checked that the circular surface area of the 8-mm diameter of pyroelectric detector is large enough to collect the whole reflected energy, by changing the inclination angle of reference mirror. All measurements are carried out in groups at room temperature. Each group includes, at most, four different samples, and the reference mirror is measured twice at the beginning and the end of each group.

When measuring the diffuse component R_D of the spectral normal-hemispherical reflectance of the sample the aperture A is fully opened, while for measuring the angular distribution of the diffuse reflection the aperture is opened at a size corresponding to the polar angle of reflection θ . The diffuse component R_D is calculated in terms of the measured detector outputs V and V^* for the sample and reference mirror, respectively, by

$$R_D = C(V/V^*)R^* \quad (2)$$

where R^* is the spectral absolute reflectance of the reference mirror. The correction factor C is introduced to account for the solid angle effect of incident hole and to correct for the shadowing by the sample holder.

The specular components R_S of the spectral normal-hemispherical reflectance of the sample is measured separately with specular reflectance attachments using double beam prism-type spectrophotometers. The value of R_S is

calculated in terms of the measured quantities M and M^* for the sample and the reference mirror, respectively, by

$$R_s = (M/M^*)R^* - xR_D \quad (3)$$

where x is a small fraction of the diffuse reflection included in the measurements of the specular component. The correction for the solid angle effect of incident hole is -0.01 and that for the shadowing effect of sample holder is -0.052 . Values of C in Eq. (2) and x in Eq. (3) are then taken to be 1.066 and 0.01, respectively. The maximum error included in this experiment is estimated to be $\pm 4\%$ of each value for R_D and R_h . The spectral normal-hemispherical reflectance R_h is, thus, given by

$$R_h = R_D + R_s \quad (4)$$

The angular distribution of the diffuse reflection is expressed by a reflection function $R(\theta_0 \sim \theta)$. It is defined as the ratio between the radiation energy diffusely reflected in the finite solid angle confined by the polar angles θ_0 and θ , and the incident radiation energy. The angle $\theta_0 = 12.4$ deg is the semiapex angle of the conical hole of the incidence, and it corresponds to the escaping portion of the diffuse reflection. Thus, $R(\theta_0 \sim \theta)$ is calculated by

$$R(\theta_0 \sim \theta) = C(\theta) [V(\theta)/V^*]R^* \quad (5)$$

where $V(\theta)$ is the detector output for an aperture opening corresponding to the angle θ . The function $C(\theta)$ is introduced to correct for the shadowing by the sample holder and calculated easily, assuming uniform diffuse reflection.

Results and Discussion

In the following the comparison is made between the experimental results and the calculated results based on the analytical techniques for calculating the scattering properties and the radiative transfer, that have been discussed in detail in Refs. 1-5. Average values of the particle diameter 0.3, 0.05, and 0.3 μm are estimated^{21,22} for the nearly spherical pigments TiO_2 , carbon, and Fe_2O_3 , respectively. For ZnO particles an average size of a square rod is estimated to be 0.1 $\mu\text{m} \times 0.1 \mu\text{m} \times 0.7 \mu\text{m}$.²¹ The thickness of the dry painted layer, which is used in the calculation, was measured with a micrometer thickness gage. For each sample, measurements were made at different points, and an average thickness L was adopted. For thin layers the value of L was checked by that estimated from the interference maxima which occur (channel spectra) in the spectrum of the specular reflectance measurements. The pigment volume concentration v of the dry layer is obtained from the following relation:

$$vL = v_w L_w \quad (6)$$

where v_w and L_w are the pigment volume concentration and the thickness of the wet layer.

It should be noted that the interference effects due to the multiple reflection of light appear in the measurements for the specular reflectance of thin painted layers ($\tau_l < 2$) on the specular substrate. These effects are observed as maxima and minima in the spectrum of the reflectance measurements commonly referred to as channel spectra. For the comparison with the analysis, the value of the measured quantity M in Eq. (3) (for the calculation of the specular component R_s) was taken to be the average over the maxima and the minima of the spectrum.

Figures 2-5 show the results for the wavelength dependence of the spectral normal-hemispherical reflectance R_h and its diffuse component R_D . The effect of the pigment volume concentration v is shown in Fig. 2 for TiO_2 -Al (specular substrate) samples having the same wet layer thickness $L_w = 50 \mu\text{m}$. The wavelength dependencies of R_D and R_h

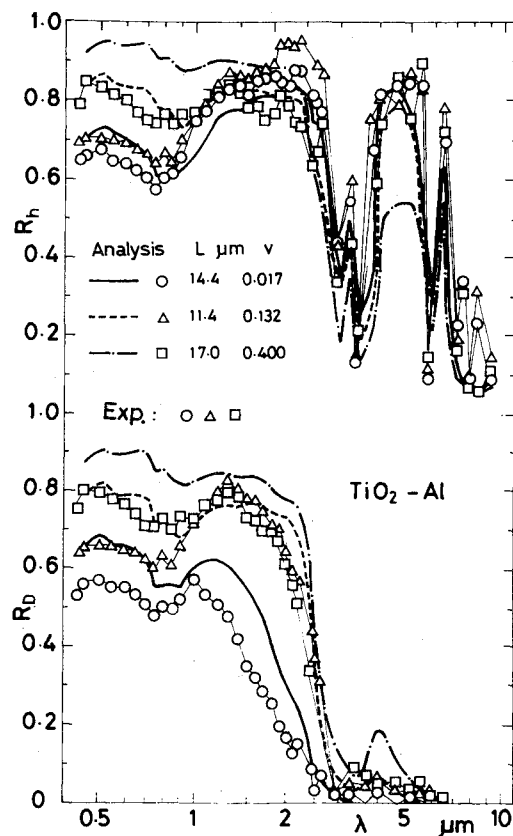


Fig. 2 Effect of the pigment volume concentration on the wavelength dependence of R_D and R_h .

predicted by theoretical calculations (Analysis) are seen to correspond closely with the experimental measurements (Exp.). For all values of the pigment volume concentration, R_D decreases much due to the decrease of the scattering properties as the wavelength λ increases. Both experiment and analysis show weak absorption bands by the vehicle in the NIR region, in the wavelength interval of $\lambda = 0.7 \sim 0.9 \mu\text{m}$, while they clearly show several strong absorption bands and peaks in the IR region. The large values of R_h in the wavelength interval of $\lambda = 4.0 \sim 5.0 \mu\text{m}$ are mainly due to the large values of the specular component corresponding to the weak absorption by the vehicle in thin layers ($L = 11.4 \sim 17.0 \mu\text{m}$) on the specular Al substrate of high reflectivity.

The diffuse component R_D increases with the increase of v in the VIS region for both the experiment and the analysis. At longer wavelengths (NIR) the experimental results show different characteristics for a large value of $v = 0.4$. This is mainly due to the enhanced effect of the interference between scattered fields of the pigment particles. This effect was neglected in the calculation for large pigment volume concentrations.¹ Previous experimental studies²³⁻²⁸ concerning the interference effect due to the small separation distance between particles have been limited to specified cases of spherical pigment, nonabsorbing dispersed medium, and short wavelengths (VIS region). The formulas derived in some of these studies to correlate the interference effect are not considered satisfactory enough to be introduced for the calculations of the general case of the painted layer. However, all these studies included the conclusion that the most important factor, for uniformly dispersed particles, is the ratio of the separation distance between the particles to the wavelength. For a large value of v and at a long wavelength this ratio decreases and a strong effect of the interference occurs, resulting in a reduction of the scattering efficiency for the single particle. Thus, it may be useful to explain the tendency of the present experimental results in the view of the preceding statement as follows. The reduction of the scat-

tering efficiency for a large value of $v=0.4$ due to the interference effect leads to small values of the optical thickness and the scattering albedo of the painted layer (in the presence of the vehicle absorption); accordingly, smaller values of R_D are found, compared with those for a smaller value of $v=0.132$. In the wavelength interval of $\lambda=4.0\sim 5.0\ \mu\text{m}$, where the contribution of the specular component R_S to R_h is large, the experiment shows larger values of R_h compared with the analysis for $v=0.4$. This is also due to the interference effect, resulting in small values of the optical thickness with large values of R_S .

In general, the experiment shows smaller values of R_D compared with the analysis. This may be attributed mainly to the interference effect, the uncertainty in determining the dense concentration v_c in Eq. (1), the error in measuring the thickness L of the dry painted layer, and the assumptions in the analysis that TiO_2 particles are exactly spherical and uniformly dispersed in the vehicle as individual particles; whereas the experiment deals with real situation of not restrictively spherical particles, resulting in smaller scattering properties.⁴ Also the agglomeration of the pigment particles in the dry layer and the nonuniform dispersion reduce the scattering of the layer.²² Examination of the results for $v=0.017$ shows that the analysis has the same wavelength dependence as the experiment; thus, the choice of $d=0.3\ \mu\text{m}$ as average-effective particle diameter for TiO_2 pigment is suitable. Therefore, the factors mentioned above lead to nearly constant reduction in the scattering properties independent of the wavelength.

Figure 3 shows the effect of the layer thickness L . Extreme cases of thin ($L=14.4, 17.0\ \mu\text{m}$) and thick ($L=274.0, 682.0\ \mu\text{m}$) layers are considered with small and large pigment volume concentrations. In the wavelength interval of $\lambda=0.45\sim 1.0\ \mu\text{m}$, the thick layers exhibit larger values of R_D and R_h compared with the thin layers of the same volume concentration for both the experiment and the analysis. As the

wavelength increases from 1.0 to $7.0\ \mu\text{m}$, the thick layer still has larger values of R_D than the corresponding thin layer of a small concentration ($v=0.017, 0.023$). While for a large concentration ($v=0.4, 0.486$) the experiment shows a different tendency. The values of R_D for the thick layer approach those for the thin layer and become smaller than them. This tendency can be explained as follows. The interference effect of scattering due to the small value of particle separation distance to wavelength ratio, together with the large absorption by the vehicle, decreases much the scattering albedo $\bar{\omega}$ for the large volume concentration. The thick layer ($L=682.0\ \mu\text{m}$) still has a large value of the optical thickness, and it behaves nearly as an infinitely optically thick layer ($\tau_l = \infty$)² for which R_D and R_h decrease with the decrease in $\bar{\omega}$. In the wavelength interval of $\lambda=4.0\sim 5.0\ \mu\text{m}$ the small absorption by the vehicle in the thin layers leads to large values of the specular component R_S and, accordingly, large values of R_h . On the other hand, the large absorption by the vehicle in the thick layers decreases R_S to the limiting value which corresponds to the first specular reflection at the air-vehicle interface, resulting in smaller values of R_h .

It should be noted that in the wavelength interval of $\lambda=0.75\sim 1.3\ \mu\text{m}$ the experiment agrees well with the analysis for both R_D and R_h of the thick layer with large pigment volume concentration. This is because the TiO_2 pigment is nonabsorbing and has large scattering efficiency factor, and the vehicle is weakly absorbing in this wavelength interval. Therefore, the optical thickness τ_l still has a large value and the scattering albedo $\bar{\omega}$ is still very close to unity even with the reduction in the scattering efficiency due to the factors discussed before.

Figure 4 shows the combined effect of the shape and the optical properties of the pigment. The results of R_D and R_h for the case of ZnO are smaller than those for the case of TiO_2 . This is mainly because ZnO has smaller real refractive indexes ($n_p=2.0$) compared with those of TiO_2 ($n_p=2.5$) in

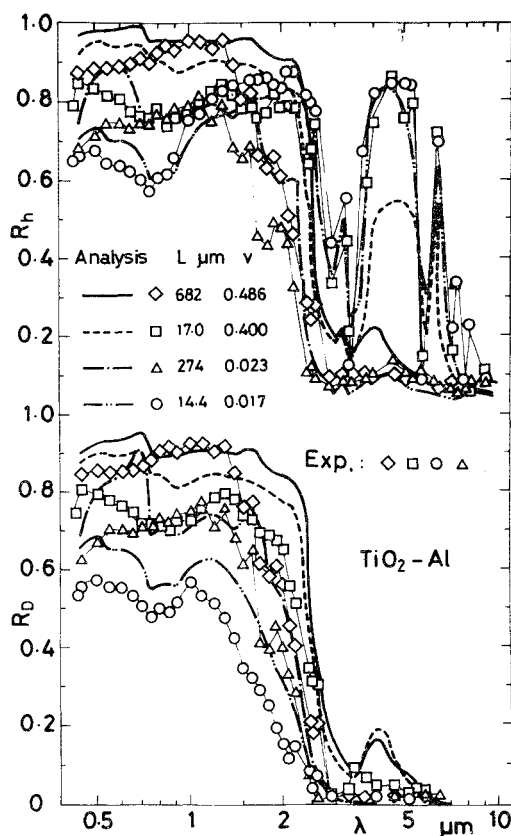


Fig. 3 Effect of the layer thickness on the wavelength dependence of R_D and R_h .

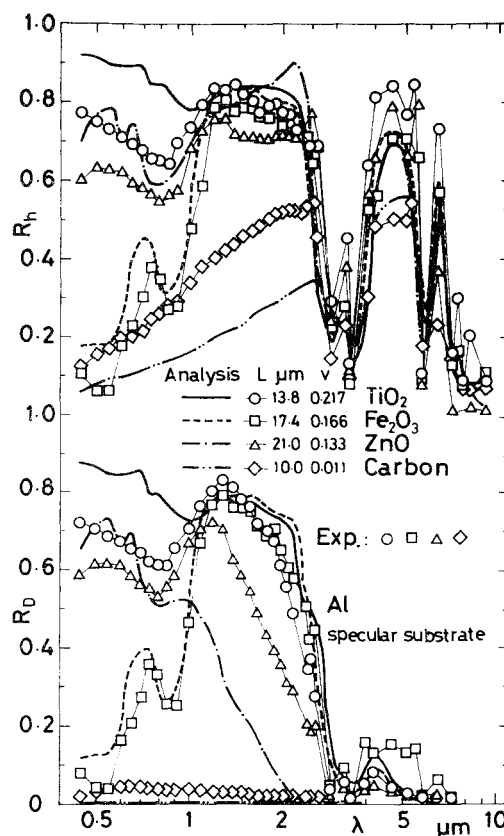


Fig. 4 Effect of the pigment properties on the wavelength dependence of R_D and R_h .

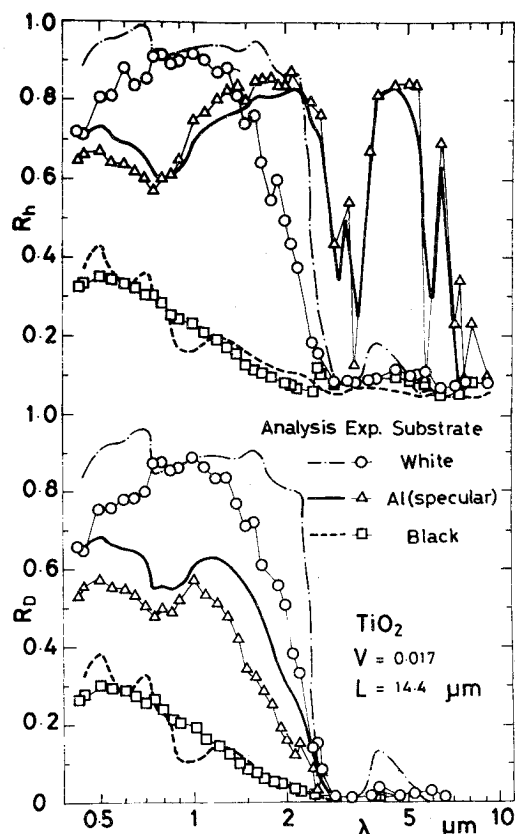


Fig. 5 Effect of the reflection characteristics of the substrate on the wavelength dependence of R_D and R_h .

the VIS and NIR regions. The shift of the R_D curve of the analysis for the case of ZnO to the shorter wavelengths relative to the experimental results may be due to the small size of the rod-like particle of ZnO considered in the analytical calculation. The large absorption efficiency of the carbon black pigment, even with small volume concentration, decreases to a large extent the values of R_D in the whole wavelength range. The absorption by Fe_2O_3 pigment in the VIS region (red color) decreases R_D in the wavelength interval of $\lambda = 0.43 \sim 0.6 \mu\text{m}$. As the absorption coefficient of Fe_2O_3 pigment decreases with the increase of the wavelength, R_D and R_h increase, and their values approach those for TiO_2 due to nearly the same scattering properties. The results of R_h for both the experiment and the analysis in the case of Fe_2O_3 are in good agreement due to the matching of the data for the analysis with the real situation. The deviation of the analysis from the experiment in the case of carbon in the VIS and NIR regions can be explained by the uncertainty in the optical constants of carbon adopted for the analysis.¹

Figure 5 shows the effect of the reflection characteristics of the substrate. The results for specular Al substrate and two other different substrates are plotted. Thick layers of densely concentrated white (TiO_2) and black (carbon) paints are used to represent highly reflecting diffuse and nearly perfectly absorbing substrates, respectively, in the VIS and NIR regions. The analytical results for the case of black substrate could be obtained by considering a substrate of zero reflectance in the vehicle side. While for the case of white substrate analytical results could be obtained by considering the problem of a doubly painted layer,⁵ and treating the white substrate as under coat of an infinite optical thickness. The values for the case of black substrate represent mainly the contribution by back scattering of the attenuated incident light, where good agreement between the analysis and the experiment could be seen. The irregularities in the wavelength dependence of the analytical results compared with the

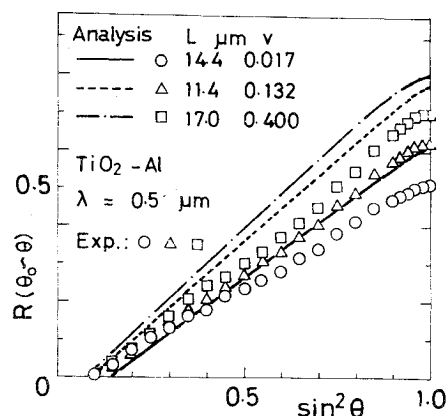


Fig. 6 Effect of the pigment volume concentration on the angular distribution of the diffuse reflection.

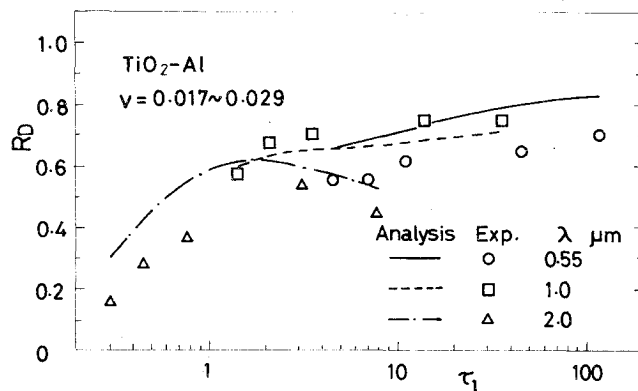


Fig. 7 τ_l dependence of the diffuse component of the spectral normal-hemispherical reflectance for TiO_2 -Al system.

smooth one for the experiment can be explained by the resonances in the spectrum of the scattering coefficient of the spherical particle according to Mie theory. In the analysis an assumption of a monodispersion of spherical particles of TiO_2 pigment is considered. Because of the small concentration ($v=0.017$) and the nearly perfect absorption by the substrate, the contribution of the multiple scattering is small and the single scattering dominates. This results in a direct correspondence of the wavelength dependence of R_D with the irregular spectrum of the scattering coefficient for single particles of $d=0.3 \mu\text{m}$. However, the experiment deals with a real situation of a polydispersion of particles having nearly an average value of $d=0.3 \mu\text{m}$, and the summing of the resonances in the spectra of the scattering coefficient for the different sizes of the spherical particles results in a smooth wavelength dependence of R_D . The clear difference between the specular and the diffuse substrates can be seen for R_h in the IR region where the specular reflection at the boundaries of the painted layer dominates.

Figure 6 shows the results for the angular distribution of the diffuse reflection. The effect of the pigment volume concentration v is shown in Fig. 6. Due to the large values of the optical thickness for large values of v (0.132, 0.4) both the experiment and the analysis show linear dependence of $R(\theta_0 \sim \theta)$ on $\sin^2 \theta$ up to a value of $\sin^2 \theta \approx 0.75$ ($\theta \approx 60^\circ$). This linear dependence represents a uniform diffuse reflection since $R(\theta_0 \sim \theta)$ expresses its integration with respect of $\sin^2 \theta$ (Ref. 1). The experiment shows clearly the slow increase in $R(\theta_0 \sim \theta)$ near $\sin^2 \theta = 1.0$, which means the decrease of the bidirectional reflectance to a zero value due to the total specular reflection in the vehicle side at the air-vehicle interface. The analysis also shows the same tendency, but it is not clear due to the numerical integration. Figures 7 and 8

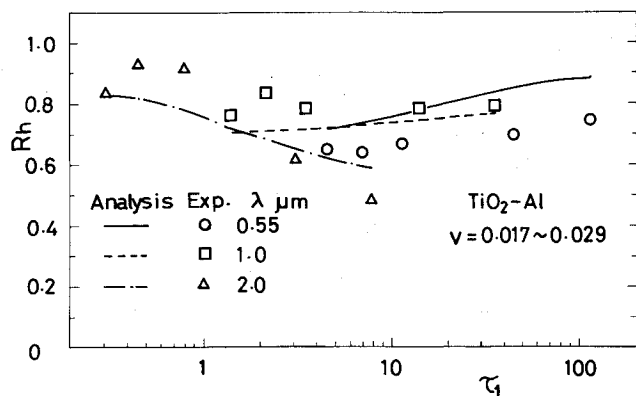


Fig. 8 τ_l dependence of the spectral normal-hemispherical reflectance for TiO_2 -Al system.

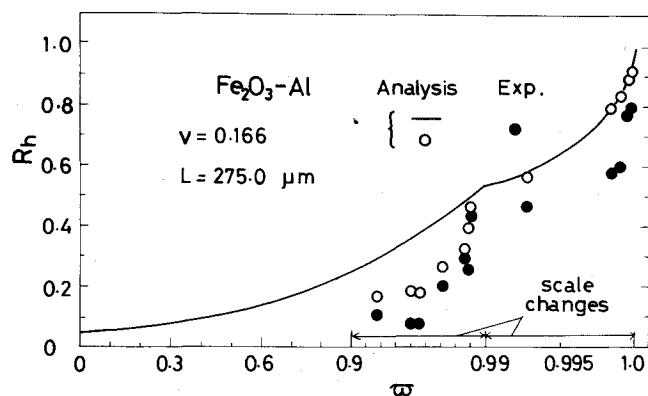


Fig. 10 The dependence of the spectral normal-hemispherical reflectance on the scattering albedo for optically thick layer (Fe_2O_3).

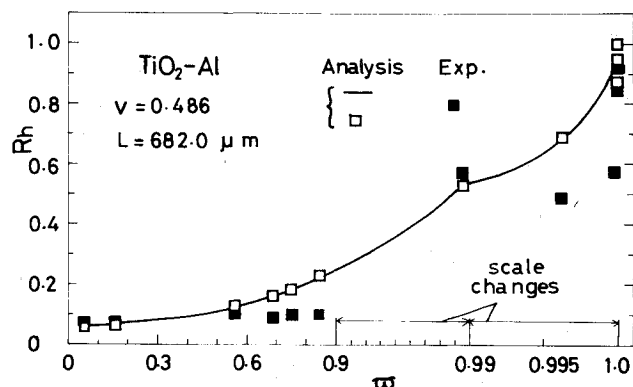


Fig. 9 The dependence of the spectral normal-hemispherical reflectance on the scattering albedo for optically thick layer (TiO_2).

show, respectively, the dependencies of R_D and R_h on the optical thickness τ_l . The results at different wavelengths are plotted to demonstrate the effect of the wavelength λ and, accordingly, the effect of the scattering albedo of the layer. The results were obtained for painted samples containing TiO_2 pigment with a wet state volume concentration $v_w = 0.005$ and having varied thicknesses ($L = 13.0 \sim 274.0 \mu\text{m}$) applied to specular Al substrate. Both the experiment and the analysis show the same tendency of the τ_l dependence at each value of λ , where the effect of the interference between the scattered fields is negligibly small due to the small volume concentration. As τ_l increases larger than unity, R_D and R_h increase continuously at $\lambda = 0.55$ and $1.0 \mu\text{m}$ and each approaches to a corresponding asymptotic value as $\tau_l \rightarrow \infty$, while they decrease at $\lambda = 2.0 \mu\text{m}$. In the case of $\lambda = 2.0 \mu\text{m}$ there is very small absorption by pigment and vehicle. This absorption effect is enhanced by the increased multiple scattering due to the large value of τ_l and reflectivities begin to decrease.²

Figures 9 and 10 show the dependence of R_h on the scattering albedo of the layer $\bar{\omega}$ for thick layers with large pigment volume concentration. The values of $\bar{\omega}$ were calculated neglecting the interference effect. The analytical curve describing the R_h vs $\bar{\omega}$ relation for an infinite optically thick layer with isotropic scattering is plotted to examine the effect of the scattering phase function.² The results for the case of TiO_2 in Fig. 9 show that nearly good agreement between the analysis and the experiment exists either at large values of $\bar{\omega}$ very close to unity or at small values ($\bar{\omega} < 0.6$). While for other values the interference effect due to the large value of ν leads to a disagreement. In the analysis the dominant forward scattering, resulting in smaller values of R_h than those of the isotropic scattering,² enhances the effect of the interference at $\bar{\omega} = 0.9997$. This also can be clearly seen in Fig. 10 for the

results of Fe_2O_3 in the range of $0.99 > \bar{\omega} > 0.9$. Excluding the deviation between the analysis and the experiment due to other factors, the effect of interference may be correlated by the reduction in the value of $\bar{\omega}$ corresponding to the shift of the experimental point to match with the analysis.

Conclusions

The experimental measurements of the various reflective properties of painted layers under the condition of normal incidence have been carried out using a new diffuse reflectometer. The comparison was made with the calculated results based on previous analyses to check the analytical procedure and to examine the various assumptions considered in the theoretical modeling. In general, the analysis shows good qualitative and quantitative agreement with the experiment except for the effect of the interference, which must be considered by a suitable correlation in the analysis at large pigment volume concentrations.

Acknowledgments

A part of this research was supported by the Grant-in-Aid for Energy Research (56040063) from the Ministry of Education, Science and Culture of Japan.

References

- Kunitomo, T., Shafey, H. M., and Teramoto, T., "Theoretical Study on Radiative Properties of a Painted Layer Containing Spherical Pigment (Case of Normal Incidence)," *Bulletin of the Japan Society of Mechanical Engineers*, Vol. 22, Nov. 1979, pp. 1587-1594.
- Shafey, H. M. and Kunitomo, T., "Theoretical Study on Radiative Properties of an Optically Thick Painted Layer Containing Spherical Pigment (Case of Normal Incidence)," *Bulletin of the Japan Society of Mechanical Engineers*, Vol. 23, Aug. 1980, pp. 1366-1373.
- Shafey, H. M. and Kunitomo, T., "Theoretical Study on Radiative Properties of a Painted Layer Containing Spherical Pigment (Cases of Oblique and Hemispherical Incidences)," *Bulletin of the Japan Society of Mechanical Engineers*, Vol. 23, Nov. 1980, pp. 1842-1848.
- Shafey, H. M. and Kunitomo, T., "Radiative Properties of a Painted Layer Containing Nonspherical Pigment," *AIAA Progress in Astronautics and Aeronautics, Heat Transfer and Thermal Control*, edited by A. L. Crosbie, Vol. 78, New York, 1981, pp. 3-24.
- Shafey, H. M. and Kunitomo, T., "Theoretical Study on Radiative Properties of Doubly Painted Layers," *Bulletin of the Japan Society of Mechanical Engineers*, Vol. 25, Feb. 1982, pp. 213-216.
- Sanderson, J. A., "The Diffuse Spectral Reflectance of Paints in the Near Infra-Red," *Journal of The Optical Society of America*, Vol. 37, Oct. 1947, pp. 771-776.
- Streed, E. R. and Beveridge, C. M., "The Study of Low Solar Absorptance Coatings for a Solar Probe Mission," *Proceedings of the Symposium on Thermal Radiation of Solids*, NASA SP-55, 1965, pp. 535-548.
- Kremininghaus, A. B., "Infrared Reflectance of Paints," *Applied Optics*, Vol. 8, April 1969, pp. 807-812.

⁹Williams, G. C. and Howard, R. R., "The Effect of Film Pigment and Substrate Colors on the Reflectance of Paint Films," *Journal of Paint Technology*, Vol. 40, May 1968, pp. 229-239.

¹⁰Billmeyer, F. W. and Carter, E. C., "Color and Appearance of Metallized Paint Films: II. Initial Application of Turbid-Medium Theory," *Journal of Coatings Technology*, Vol. 48, Feb. 1976, pp. 53-60.

¹¹Johnston-Feller, R. and Osmer, D., "Exposure Evaluation: Quantification of Changes in Appearance of Pigmented Materials," *Journal of Coatings Technology*, Vol. 49, Feb. 1977, pp. 25-36.

¹²Hislop, R. W. and McGinley, P. L., "Microvoid Coatings: Pigmented, Vesiculated Beads in Flat Latex Paints," *Journal of Coatings Technology*, Vol. 50, July 1978, pp. 69-77.

¹³Touloukian, Y. S. and DeWitt, D. P., *Thermophysical Properties of Matter, Vol. 8: Thermal Radiation Properties; Nonmetallic Solids*, IFI/Plenum, New York, 1972, pp. 32a-39a.

¹⁴Eckert, E. R. G. and Goldstein, R. J., *Measurements in Heat Transfer*, Hemisphere Publishing Corporation, Washington, D. C., 1976, Chap. 10.

¹⁵Finkel, M. W., "Portable Reflectometer," *AIAA Progress in Astronautics and Aeronautics. Thermophysics: Applications to Thermal Design of Spacecraft*, edited by Jerry T. Bevens, Vol. 23, Academic Press, New York, 1970, pp. 65-75.

¹⁶Gier, J. T., Dunkle, R. V., and Bevens, J. T., "Measurements of Absolute Spectral Reflectivity from 1.0 to 15 Microns," *Journal of the Optical Society of America*, Vol. 44, July 1954, pp. 558-562.

¹⁷White, J. U., "New Method for Measuring Diffuse Reflectance in the Infrared," *Journal of the Optical Society of America*, Vol. 54, Nov. 1964, pp. 1332-1337.

¹⁸Blevin, W. R. and Brown, W. J., "An Infrared Reflectometer

with a Spheroidal Mirror," *Journal of Scientific Instruments*, Vol. 42, April 1965, pp. 385-389.

¹⁹Neher, R. T. and Edwards, D. K., "Far Infrared Reflectometer for Imperfectly Diffuse Specimens," *Applied Optics*, Vol. 4, July 1965, pp. 775-780.

²⁰Strong, J., *Procedures in Experimental Physics*, Prentice Hall, 1938.

²¹Society of Powder Technology, Japanese Cooperation of Powder Industry, *Powder Properties: Illustration by Figures*, Production Engineering Pub. Center, Tokyo, 1975 (in Japanese).

²²Dunn, E. J., Swartz, H. E., Baier, C. H., and Zuccarello, R. K., "Agglomeration of Pigment Particles in Dried Paint Films," *Journal of Paint Technology*, Vol. 40, March 1968, pp. 112-122.

²³Blevin, W. R. and Brown, W. J., "Effect of Particle Separation on the Reflectance of Semi-Infinite Diffusers," *Journal of the Optical Society of America*, Vol. 51, Feb. 1961, pp. 129-134.

²⁴Londergan, M. C. and Spengeman, W. F., "Modern Titanium Dioxide Pigments," *Journal of Paint Technology*, Vol. 42, April 1970, pp. 260-264.

²⁵Hottel, H. C., Sarofim, A. F., Vasalos, I. A., and Dalzell, W. H., "Multiple Scatter: Comparison of Theory with Experiment," *Journal of Heat Transfer*, Vol. 92, May 1970, pp. 285-291.

²⁶Hottel, H. C., Sarofim, A. F., Dalzell, W. H., and Vasalos, I. A., "Optical Properties of Coatings. Effect of Pigment Concentration," *AIAA Journal*, Vol. 9, Oct. 1971, pp. 1895-1898.

²⁷Tunstall, D. F. and Hird, M. J., "Effect of Particle Crowding on Scattering Power of TiO₂ Pigments," *Journal of Paint Technology*, Vol. 46, Jan. 1974, pp. 33-40.

²⁸Marcus, R. T. and Welker, J., "Pigment Volume Concentration Effects in Color Prediction and Practice," *Journal of Coatings Technology*, Vol. 50, July 1978, pp. 78-83.

AIAA Meetings of Interest to Journal Readers*

Date	Meeting (Issue of AIAA Bulletin in which program will appear)	Location	Call for Papers†	Abstract Deadline
1983				
Jan. 10-13	AIAA 21st Aerospace Sciences Meeting (Nov.)	MGM Grand Hotel Reno, Nev.	April 82	July 6, 82
April 11-13	AIAA 8th Aeroacoustics Conference (Feb)	Terrace Garden Inn Atlanta, Ga.	July/Aug. 82	Oct. 1, 82
May 10-12	AIAA/ASME/ASCE/AHS 24th Structures, Structural Dynamics & Materials Conference (Mar.)	Sahara Hotel Lake Tahoe, Nev.	June 82	Aug. 31, 82
May 10-12	AIAA Annual Meeting and Technical Display	Long Beach Convention Center Long Beach, Calif.		
June 1-3	AIAA 18th Thermophysics Conference (Apr.)	The Queen Elizabeth Hotel, Montreal, Quebec, Canada	Sept. 82	Dec. 1, 82
June 27-29	AIAA/SAE/ASME 19th Joint Propulsion Conference and Technical Display (Apr.)	Westin Hotel Seattle, Wash.	Sept. 82	Dec. 7, 82
July 12-14	AIAA 16th Fluid and Plasma Dynamics Conference (May)	Radisson Ferncroft Hotel and Country Club, Danvers, Mass.	Oct. 82	
July 13-15	AIAA 6th Computational Fluid Dynamics Conference (May)	Radisson Ferncroft Hotel and Country Club, Danvers, Mass.	Oct. 82	
July 13-15	AIAA Applied Aerodynamics Conference (May)	Radisson Ferncroft Hotel and Country Club, Danvers, Mass.	Oct. 82	

*For a complete listing of AIAA meetings, see the current issue of the AIAA Bulletin.

†Issue of AIAA Bulletin in which Call for Papers appeared.

‡Cosponsored by AIAA. For program information, write to: AIAA Meetings Department, 1290 Avenue of the Americas, New York, N.Y. 10104.